Aerosol and Air Quality Research, 16: 1118–1130, 2016

ISSN: 1680-8584 print / 2071-1409 online
doi: 10.4209/aaqr.2015.06.0407

Airborne Measurements of High Pollutant Concentration Events in the Free Troposphere over the West Coast of South Korea between 1997 and 2011

Greem Lee[1], Hye-Ryun Oh[1], Chang-Hoi Ho[1*], Jinwon Kim[2], Chang-Keun Song[3], Lim-Seok Chang[3], Jae-Bum Lee[3], Seungmin Lee[4]

[1] *School of Earth and Environmental Sciences, Seoul National University, Seoul, Korea*
[2] *Department of Atmospheric and Oceanic Sciences, UCLA, Los Angeles, California, USA*
[3] *Air Quality Research Division, National Institute of Environmental Research, Incheon, Korea*
[4] *Korea Environment Institute, Sejong, Korea*

ABSTRACT

Aircrafts enable the direct measurement of chemical components in the free troposphere (FT). This study employed airborne measurements to examine the occurrences of high concentrations of SO_2 and NO_x in the FT over the coastal region west of the Seoul metropolitan area, South Korea. The data from a long-term (1997–2011) airborne measurement campaign were used to determine the meteorological conditions favorable for carrying these pollutants into the Seoul area. The back trajectory analyses of 21 instances of high FT pollutant concentration events showed ascending patterns from the major pollutant sources, mainly the industrial complexes in eastern China, in 9 instances and passing patterns in 12 instances. In the ascending instances, developing low-pressure systems over the source regions provide favorable conditions to uplift air pollutants from the surface into the FT. In the passing instances, an anomalous low-pressure system near the surface prevented airflows from descending into the boundary layer and upper-level anticyclonic systems helped to keep the ascending airflows in the FT. This study proposes the basic mechanisms for predicting air quality in the Seoul area, considering that air pollutants in the FT often entrain into the boundary layer to increase local concentrations.

Keywords: Seoul; Aircraft measurement; Free troposphere; SO_2; NO_x.

INTRODUCTION

Air pollutants from industrial sources adversely affect the health of humans and ecosystems, deteriorate facilities, and cause traffic problems by the reduced visibility. Because of the health risk, the World Health Organization (WHO) has developed an air quality guideline to provide the thresholds for health-harmful pollution levels (World Health Organization, 2006). Additionally, a number of countries have also developed their own standards to regulate the ambient air quality. China has limited the emissions of major pollutants since 1982 and is planning to implement more stringent air quality standards nationwide for 10 pollutants including sulfur dioxide (SO_2), nitrogen dioxide (NO_2), nitrogen oxides (NO_x), carbon monoxide (CO), ozone (O_3), particulate matter with diameter $\leq$ 10 μm (PM_{10}) and $\leq$ 2.5 μm ($PM_{2.5}$), total suspended particles, lead (Pb), and benzopyrene, by 2016 (China MEP, 2012). The limit for NO_2 (200 μg m^{-3} in the 1-h average) in cities in China is the same as that of the WHO guideline, whereas the limits for other gases differ. The limit for SO_2 in China (WHO) is 150 (20) μg m^{-3} in the 24-h average, for O_3 it is 160 (100) μg m^{-3} in the 8-h average, and for PM_{10} and $PM_{2.5}$ it is 150 (50) μg m^{-3} and 75 (25) μg m^{-3} in the 24-h average, respectively. It is clear that the current air quality standards in China are relatively loose compared with those of the WHO. Moreover, while the total emissions of SO_2 in China began to decrease after 2006 (Lu *et al.*, 2010), the total emissions of NO_x in China have tripled during the period 1980–2010 (Liu *et al.*, 2013). In 2010, the anthropogenic emissions of NO_x were estimated at 26.06 Mt, an increase of 33.8% from 2005 (Zhao *et al.*, 2013), attributable to the rapid growth of industries and the increase in transportation.

As the Korean peninsula is located generally downwind of China, the concentrations of air pollutants in many of the metropolitan areas in Korea are affected not only by the local emissions but also by the remote emissions in China. The west coastal region of Korea has been targeted for the monitoring of air pollutant concentrations and flow patterns for longer than a decade (e.g., Choi *et al.*, 2001; Kim *et al.*, 2007; Noh *et al.*, 2007; Koo *et al.*, 2008; Lee *et al.*, 2013) to quantify the transboundary transport of pollutants from

* Corresponding author.
Tel.: 82-2-880-8861; Fax: 82-2-876-6795
E-mail address: hoch@cpl.snu.ac.kr

China, with minimal effect from the local emissions. A number of studies have analyzed the air pollutants transported in the planetary boundary layer (PBL). However, the significance of air pollutants in the free troposphere (FT) should also be emphasized, as air pollutants in the FT influence radiative transfer and are often transported downstream over large distances (Heald *et al.*, 2005; Zhu *et al.*, 2007; He *et al.*, 2012). These pollutants often descend into the PBL and cause adverse effects on the air quality in remote regions and, consequently, on human health (Heald *et al.*, 2006; Colette *et al.*, 2008; Cooper *et al.*, 2010).

Despite the importance of the FT pollutant transport in assessing the regional air quality, in-situ air pollutants measurements in the FT are rare. Data from satellites or lidar suffer from relatively large uncertainties due to the indirect measurements of the concentrations of air pollutants in the troposphere [for example, the Multi-angle Imaging SpectroRadiometer derives an aerosol optical depth over global land with an uncertainty of ~20% (Yu *et al.*, 2006), and the Raman lidar can measure the profiles of aerosol extinction with uncertainty of 15–20% (Schmid *et al.*, 2009)]; the distribution of chemical components from satellite have been retrieved from calibrated radiances (Deeter *et al.*, 2003; Waters *et al.*, 2006; Clerbaux *et al.*, 2009) and lidar has detected aerosols with the aerosol optical properties such as backscatter coefficient and extinction coefficient (Welton *et al.*, 2000; Müller *et al.*, 2007). In situ airborne observations are useful for measuring the air pollutants for two reasons. Firstly, the global positioning system of the aircraft samples the vertical profiles of air pollutants with accurate geographical reference, making it possible to separate the distribution of the chemical components between the PBL and the FT if the PBL height is known. Secondly, the concentration of specific components, such as SO_2, CO, O_3, NO_x, etc. directly measured from the aircraft, facilitates quantitative analysis (e.g., Hatakeyama *et al.*, 2004; Corrigan *et al.*, 2008; Wang *et al.*, 2008; Chen *et al.*, 2013; Zhang *et al.*, 2014). Airborne measurements allow to distinguish the FT air pollutants from those in the PBL, and in turn allow to identify the meteorological conditions related with the occurrence of high-concentration events in the troposphere. This is very useful for improving the prediction of air quality after the descent of the airstream from the FT into the PBL.

In this study, we have analyzed airborne pollutant measurements and meteorological conditions in order to understand the mechanisms by which air pollutants are uplifted into and transported within the FT. As we focus on the pollutant transport into the Seoul metropolitan areas in Korea from their upstream regions, mainly China, with minimal impacts from the local emissions from the metropolitan area in Korea, we have selected the measurements over the coastal region to the west of Seoul, i.e., the eastern parts of the Yellow Sea, for analyses. First, we have identified the instances of high pollutant concentrations above the PBL by examining the vertical distributions of the airborne pollutant measurements over the west coastal region for the period 1997–2011. We have examined the pressure patterns favorable for the injection of air pollutants into the FT and for transport of the injected air pollutants within the FT. Recent studies (Jaffe *et al.*, 1999; Tsutsumi *et al.*, 2003; Mari *et al.*, 2004) examined the effects of extratropical cyclones on the vertical transport of air pollutants in East Asia. It has been suggested that warm conveyor belts may play a major role in the vertical redistribution of air pollutants (Jacob *et al.*, 2003; Miyazaki *et al.*, 2003; Dickerson *et al.*, 2007; Ding *et al.*, 2009). Here, we show that the early-stage developing low-pressure systems can also uplift air pollutants into the FT.

Data and the analysis methodology are presented below. It is followed by analyses of the vertical distributions of SO_2 and NO_x from the airborne measurements and the pressure patterns favorable for inflow and transport of air pollutants in the FT. Summary follows the analysis section.

DATA AND METHOD

The airborne air pollutant measurement data used in this study were provided from the National Institute of Environmental Research (National Institute of Environmental Research, 2000–2010; Kim *et al.*, 2001; National Institute of Environmental Research, 2011). The data were measured on two aircraft platforms, the Chieftain PA-31-350 (Piper Aircraft, Inc., USA) used during 1997–2009 and November 2010, and King Air C90GT (Raytheon Co., USA) used during May 2010 and 2011. Two components (SO_2 and NO_x) have been selected for further study from the seven components [SO_2, CO, O_3, NO_x (NO and NO_2), NO_y, volatile organic compounds (VOCs), and the peroxyacetyl nitrate (PAN)] in the measurements. These two components (SO_2 and NO_x) are primary pollutants produced directly in urban areas and industrial complexes, and that their concentrations are closely correlated with particulate matters (Vardoulakis and Kassomenos, 2008). These gases have been measured over a long period and, in several instances, high concentrations in the FT have been detected. SO_2 and NO_x were measured by the ultraviolet fluorescence method and the chemiluminescence/photolytic converter method, respectively. These two gases were routinely calibrated with the span gases. Detection limits for SO_2 and NO_x are 0.2 ppb for the case of 10-s average and 0.05 ppb for the case of 2-min average, respectively. All calibrations were performed through the complete Teflon inlet line. The concentrations of the two gases were averaged over one-minute intervals. We have examined a total of 100 instances of the concentrations of SO_2 and NO_x measured above the PBL over the west coastal region of South Korea. The aircraft took off from Gimpo International Airport, Taean airfield, and Muan International Airport (see Fig. 1(a) for these locations). The observation area is located over the eastern region of the Yellow Sea (32.64°N–37.67°N, 124.09°E–127.37°E) with the altitude range below the 5 km level. More details of the aircraft measurements can be found in Kim *et al.* (2001).

The air quality standards of Seoul have been applied as the threshold values in selecting the instances of high concentrations of SO_2 or NO_x (http://cleanair.seoul.go.kr/main.htm). The annual (24-hour) mean threshold values of SO_2 and NO_2 (the air quality standards of Seoul do not include the threshold value for NO_x) are 10 (40) ppb and

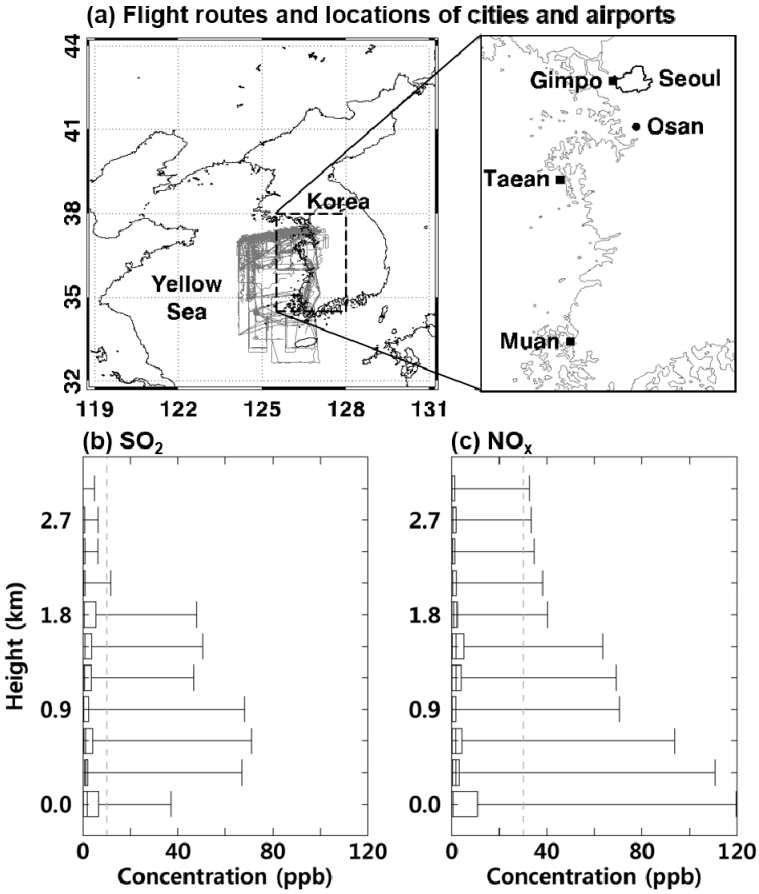

Fig. 1. The flight routes (a) and the concentrations of SO_2 (b) and NO_x (c) in 100 instances, observed over the western coastal region of South Korea. The center line of each box plot shows the 50th percentile (median) value and the box encompasses the 25th and 75th percentile of the data. Error bars mark the minimum and maximum values. A black dot in (a) denotes the Osan site. The gray dashed lines in (b) and (c) represent the air quality standards of Seoul (SO_2 > 10 ppb, NO_x > 30 ppb).

30 (60) ppb, respectively. We used the annual mean threshold values because the concentrations of air pollutants in the FT are lower than those in the PBL due to the distance from the sources and limited detrainment from the PBL. The SO_2 threshold of Seoul is 10 ppb lower than that of the national standard, while the NO_2 threshold is the same as that of the national standard. Twenty-one events (19 days) were selected as instances of high concentration in the FT. The daily SO_2 and NO_2 data from 27 air quality monitoring stations in Seoul for the same days have been used to compare the concentrations in the FT over the coastal region to the west of the metropolitan area with the surface concentrations in Seoul. Currently, the surface stations measure SO_2 and NO_2 using the ultraviolet fluorescence method and the chemiluminescence method, respectively (Seoul Metropolitan Environment, 2014).

The PBL height was calculated using the sounding data at the Osan radiosonde site located about 30 km inland of the west coast of Korea (Department of Atmospheric Science, the University of Wyoming: http://weather.uwyo.edu/upperair/sounding.html). The upper-air sounding is performed four times a day (at 00, 06, 12, and 18 UTC); we analyzed the data at 00 and 06 UTC. The bulk Richardson number (Ri) method was applied for the calculation of the PBL height (Kim and Mahrt, 1992; Vogelezang and Holtslag, 1996; Seidel *et al.*, 2012). The Ri, the ratio between the suppression/enhancement of turbulence due to buoyancy and the generation of turbulence via vertical shear, is calculated as follows

$$\mathrm{Ri} = \frac{\left(\frac{g}{\theta_{vs}}\right)\left(\theta_{vz} - \theta_{vs}\right)\left(z - z_s\right)}{\left(u_z - u_s\right)^2 + \left(v_z - v_s\right)^2} \quad (1)$$

where z is the height, the subscript s stands for the surface, g the gravitational acceleration, θ_v the virtual potential temperature, and u and v are the zonal and meridional wind speed, respectively. If Ri exceeds the critical value of 0.25 (i.e., turbulence generation by wind shear is less than the suppression by buoyancy), mechanical production cannot sustain turbulence in a stably-stratified layer (Holton, 2004). The lowest level z at which the interpolated Ri crosses 0.25, $z(Ri_{0.25})$, is the PBL height. Because of the stable stratification during the night and an explosive

growth of the PBL into the residual layer for growing mixed layer, calculations using the 00 UTC (9 a.m. local time) measurements often underestimate the PBL heights. In addition, the use of the critical Ri, estimation of the surface wind speed, the interpolation of the Ri profile, and the vertical resolution of the sounding data can induce large uncertainty in calculating the PBL heights when the PBL is thin [$z(Ri_{0.25}) < 1$ km] (Seidel *et al.*, 2012; Kretschmer *et al.*, 2014). Despite these uncertainties, we decided to use the bulk Ri method because it is suitable for both stable and convective boundary layers, identifies a nonnegative height in all cases, is not strongly dependent on the vertical resolution of soundings, and is suitable for application to large data sets. In an effort to reduce uncertainties, we have used the radiosonde data to cross-check the height of the mixed-layer top, where the vertical profiles of the potential temperature, the mixing ratio, and the wind direction and speed change abruptly (not shown).

Weather maps obtained from the Korean Meteorological Administration (KMA), were used to examine the meteorological conditions related to the ascent of the air pollutants. The domain of the maps provided by the KMA covers East Asia at a 12-hour time interval. The geopotential height on 1000, 850, 700, and 500 hPa, obtained from the National Centers for Environmental Prediction-Department of Energy (NCEP-DOE) Reanalysis 2 (Kanamitsu *et al.*, 2002), with a longitude-latitude resolution of 2.5° × 2.5°, was used to examine the meteorological conditions related to the transport of air pollutants in the FT. Anomalies of geopotential height against monthly climatology were used to exclude seasonality, as airborne measurements were conducted during all the seasons.

The back and forward trajectories of airflows were calculated by using the National Oceanic and Atmospheric Administration (NOAA) Hybrid Single-Particle Lagrangian Integrated Trajectory (HYSPLIT) model (https://ready.arl.noaa.gov/HYSPLIT_traj.php) (Draxler and Rolph, 2015). The National Centers for Environmental Prediction-National Center for Atmospheric Research (NCEP-NCAR) reanalysis data (temperature, geopotential height, pressure at the surface, and horizontal and vertical wind) were used as the input for calculating the transport of air parcels. The 72-hour back and forward trajectories were performed with a 1-hour time interval for the levels above the PBL.

RESULTS

Vertical Profiles of SO_2 and NO_x

The number of airborne observations, 100, in the FT over the west coastal region of South Korea was five times as large as those over the east- and south coastal region, given that the air pollutants emitted in the industrial regions in China are transported over the Yellow Sea into the Korean peninsula (Kotamarthi and Carmichael, 1990; Xiao *et al.*, 1997; Lee *et al.*, 2008; Lee *et al.*, 2014). Among the 100 flights (Fig. 1(a)), 32, 3, 56, and 9 flights were carried out during spring, summer, autumn, and winter, respectively. Figs. 1(b) and 1(c) describe the vertical profiles of SO_2 and NO_x for the total instances, respectively. The amounts of SO_2 and NO_x decrease with height, implying that the source regions were located at ground level. Given that the mean PBL height in Osan is approximately 1000–1500 m (Lee *et al.*, 2013, 2014), the concentrations of SO_2 and NO_x exceed the air quality threshold values (gray lines in Figs. 1(b) and 1(c)) above the PBL. The highest elevations where SO_2 and NO_x exceed the threshold values are 2200 m and 3150 m, respectively.

To select the instances of high concentrations of SO_2 or NO_x occurring in the FT, the PBL height was calculated as presented in the DATA AND METHOD section and cross-examined against the observed air pollutant profiles. The observed concentrations of SO_2 or NO_x above the PBL exceeded the air quality standards in 21 instances (19 days) over the coastal region west of the Seoul metropolitan area. Table 1 lists the flight dates, chemical components, back trajectory patterns (will be discussed in the legend of Fig. 2), the PBL height at Osan, and the mean concentrations of SO_2 and NO_x. In the FT, high concentrations mainly occurred during autumn and spring (16 and 4 instances), corresponding to 29% and 13%, respectively, of the total instances measured in the FT. The 25th percentile, median, and 75th percentile of SO_2 in 21 instances (100 cases in Fig. 1) are 0.80 (0.50) ppb, 2.41 (1.60) ppb, and 9.64 (4.20) ppb, respectively, and those of NO_x are 0.52 (0.32) ppb, 2.45 (1.72) ppb, and 7.82 (3.68) ppb, respectively. The correlation coefficients between the mean concentrations of SO_2 and NO_x (NO_2 in Seoul) measured by the aircraft and at the Seoul ground station are 0.12 and –0.20, respectively, indicating that the concentrations of these gases in the FT are not related with the surface concentrations in Seoul. In addition, this finding strongly implies that the FT air pollutant concentrations must be measured directly, not to be extrapolated from the surface values (Corrigan *et al.*, 2008).

Back trajectory analysis is useful to identify the source regions of the FT air pollutants, since the primary pollutants rise from the ground where large cities and industrial complexes are located and are minimally affected by photochemical reactions within the atmosphere. Back trajectory analyses over 72-hour periods were performed for 21 events to identify the source regions of these events of high concentrations of SO_2 and NO_x in the FT (Fig. 2). The location, height, and time of each starting point are set as the center of the flight route, the flight altitude above the PBL, and the hour when the measurements are started, respectively. We categorized 21 back trajectories into two groups to classify airflow patterns with the categorization contingent upon the ascent of airflows from the ground into the FT level. The back trajectories show ascending patterns from the ground in 9 instances and passing patterns through the FT in 12 instances. In the ascending group, airflows descended to the surface of major source regions, then rose up into the FT (Figs. 2(a) and 2(b)), suggesting the transport of surface pollutants into the FT. Note that these updrafts mostly occurs over eastern China (Fig. 2(a)). Most airflows arrived at the observation areas one to three days after the uplift except in a single case (October 10, 2008) when the airflow stayed in the FT over eastern China for six days (figure not shown). In the passing group, airflows move

Table 1. Date, chemical components, PBL height of Osan, airborne-measured concentrations of SO_2 and NO_x, and concentrations of SO_2 and NO_2 in Seoul, pertaining to the instances of the concentrations of SO_2 or NO_x in the FT exceeding the air quality standards of Seoul.

Date	Chemical components[a]	Pattern of back trajectory	PBL height of Osan (m)	Aircraft-measured concentrations (ppb)		Concentrations in Seoul (ppb)	
				SO_2	NO_x	SO_2	NO_2
1997-10-03 (a.m.)	O_3, NO_x (NO_x)	ascending	95.72	-	38.32	9.00	38.00
1997-10-03 (p.m.)	O_3, NO_x (NO_x)	passing	1693.46	-	35.90		
1997-10-05 (a.m.)	SO_2, O_3, NO_x (NO_x)	passing	95.30	1.27	26.63	5.00	26.00
1997-10-05 (p.m.)	SO_2, O_3, NO_x (NO_x)	passing	1699.93	-	27.43		
1998-11-10 (p.m.)	SO_2, O_3, NO_x (SO_2,)	passing	55.05	16.80	0.59	6.00	24.00
2000-11-18 (a.m.)	SO_2, O_3, NO_x (NO_x)	passing	52.02	0.16	32.53	7.00	34.00
2003-11-14 (p.m.)	SO_2, O_3, NO_2 (NO_2)	passing	809.83	0.36	4.19	5.32	46.53
2003-11-17 (p.m.)	SO_2, O_3, NO_2 (NO_2)	passing	498.07	0.45	0.18	5.26	45.52
2006-06-16 (a.m.)	SO_2, CO, O_3, NO, NO_2, NO_x (SO_2, NO_x)	ascending	114.54	4.28	5.06	4.01	37.09
2007-04-18 (p.m.)	SO_2, CO, O_3, NO, NO_x (SO_2, NO_x)	ascending	893.46	4.86	1.33	6.03	48.26
2007-10-18 (p.m.)	SO_2, CO, O_3, NO, NO_2, NO_x (NO_x)	passing	1004.83	2.51	44.86	4.59	43.86
2007-10-21 (a.m.)	SO_2, CO, O_3, NO, NO_2, NO_x (SO_2)	ascending	104.32	3.98	2.46	4.84	35.48
2007-10-22 (p.m.)	SO_2, CO, O_3, NO, NO_2, NO_x (SO_2)	passing	1437.71	11.16	3.36	6.14	48.69
2008-05-20 (p.m.)	SO_2, CO, O_3, NO, NO_2, NO_x, VOCs (SO_2)	ascending	60.10	3.26	2.86	5.19	42.47
2008-05-22 (p.m.)	SO_2, CO, O_3, NO, NO_2, NO_x, VOCs (SO_2)	passing	1282.13	3.08	2.90	5.64	35.81
2008-05-26 (p.m.)	SO_2, CO, O_3, NO, NO_2, NO_x, VOCs (SO_2)	passing	647.59	1.29	2.20	5.20	44.29
2008-10-10 (p.m.)	SO_2, CO, O_3, NO, NO_2, NO_x, VOCs (SO_2)	ascending	78.35	4.50	1.40	6.49	41.52
2008-10-17 (p.m.)	SO_2, CO, O_3, NO, NO_2, NO_x, VOCs (SO_2)	ascending	86.23	7.50	2.57	7.98	72.66
2010-11-15 (p.m.)	SO_2, CO, O_3, NO_2, NO_x (SO_2)	passing	963.87	41.13	0.14	5.00	20.00
2010-11-18 (a.m.)	SO_2, CO, O_3, NO_2, NO_x, VOCs (SO_2)	ascending	52.94	22.87	0.23	7.00	53.00
2010-11-20 (a.m.)	SO_2, CO, O_3, NO_2, NO_x, VOCs (SO_2)	ascending	52.38	60.50	0.26	6.00	55.00

[a] Concentrations of chemical components in parentheses exceeded air quality standards of Seoul in the FT.

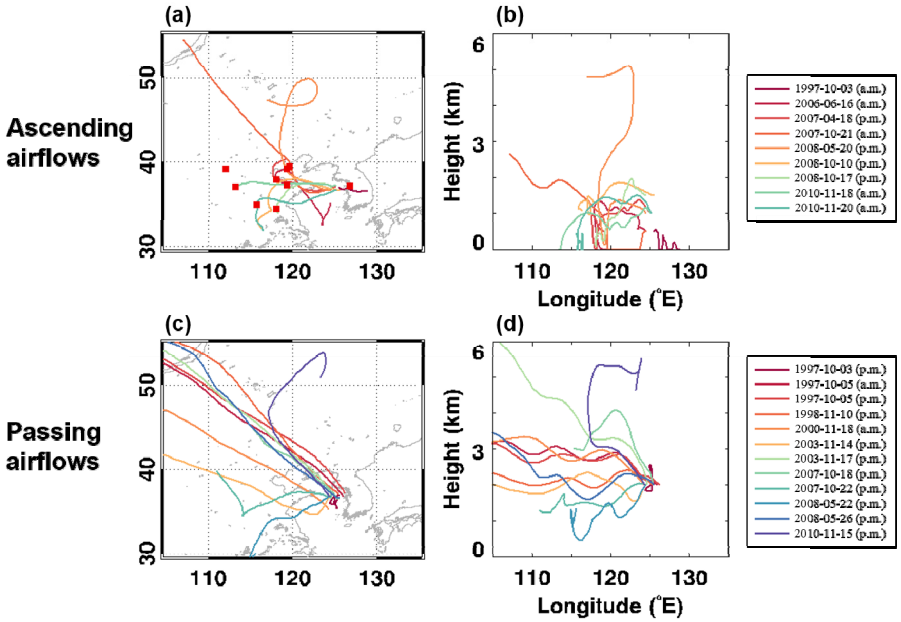

Fig. 2. The 72-hr back trajectories of the ascending airflows from the major pollution sources (a, b) and the passing airflows through the upper atmosphere (c, d). The red squares in (a) denote the updraft areas of the airflows.

through the FT faster than those in the ascending group, and there is no contact with the ground (Figs. 2(c) and 2(d)). Fig. 2(c) shows that these trajectories are mainly northwesterlies with some instances of southwesterlies. Fig. 2(d) shows the trajectories with the arrival height at 2000 m; the trajectories calculated for the other arrival altitudes above the PBL show similar features. As the lifetime of SO_2 at northern midlatitudes is 0.67–1.67 days exhibiting

seasonal variation (Chin *et al.*, 1996; Lee *et al.*, 2011) and that of NO_x is 1 day (Prather *et al.*, 2001), part of the amount of observed SO_2 and NO_x might be from the local emission. The distance between the Korean peninsula and eastern China and the fast transport of air pollutants in the FT, however, supports the fact that air pollutants emitted in China are transported into Korea. Note that the back trajectories from the HYSPLIT model may not correspond exactly with the pathways of the air pollutants since the emissions and depositions of air pollutants along the trajectories were not taken into consideration (Lee *et al.*, 2011) and the pollutants with high concentration observed from the aircraft might have stayed afloat for a long time over northeastern Asia.

The flight routes for the ascending and passing groups in Figs. 3(a) and 3(d) show that the airborne measurements focused on the instances where the flights were conducted over the coastal region west of the metropolitan area. To compare the vertical distributions of SO_2 and NO_x, their FT profiles that exceeded the air quality standards for the ascending and passing airflows are described, using box plots (Figs. 3(b), 3(c), 3(e), and 3(f)). The amounts of SO_2 and NO_x in the ascending group tend to decrease with height, whereas the concentration of SO_2 in the passing group increases with height and that of NO_x is high at the middle layer. For the ascending group, the mean concentrations of SO_2 and NO_x below (above) median height are 51.0 (31.6) ppb and 47.3 (39.3) ppb, respectively. These distributions imply that the air pollutants might only reach a limited height after the ascent from the ground level. For the passing group, the mean concentrations of SO_2 below (above) the median height are 35.0 (39.4) ppb, whereas those of NO_x are 37.7 (32.7) ppb. Note that a high NO_x concentration occurred at the 3152 m level. These suggest that air pollutants can be lifted up into higher altitudes from the source regions and can be transported far downstream over thousands of kilometers, which is similar to the characteristics of the case that He *et al.* (2012) analyzed. Note that peroxyacetyl nitrate (PAN) is produced at the expense of NO_x, and then during the long range transport, as the air parcel descends, PAN is reconverted into NO_x due to adiabatic increase of the air temperature (Hess and Vukicevic, 2003). Considering that the airflows descended more than 1 km in 8 of the passing group (Fig. 2(d)), there is possibility that NO_x was transported as PAN in the FT and decomposed as it came down to the observation altitude. The mean PBL heights over the Osan site at 06/00 UTC (i.e., 15 p.m./9 a.m. local time) for the ascending and passing groups are 279.5/84.0 m and 1009.3/73.7 m, respectively. The higher daytime PBL heights for the latter group mean that the passing airflows were located at higher altitudes.

Ascending airflows contain larger amount of air pollutants than the passing airflows. The mean concentrations of SO_2 and NO_x for the ascending (passing) group are 41.23 (37.12) ppb and 43.26 (35.19) ppb, respectively. These figures show a relatively short time for moving into the observation areas after the uplift enabled airflows to hold more air pollutants, whereas pollutants that have transferred for a longer time

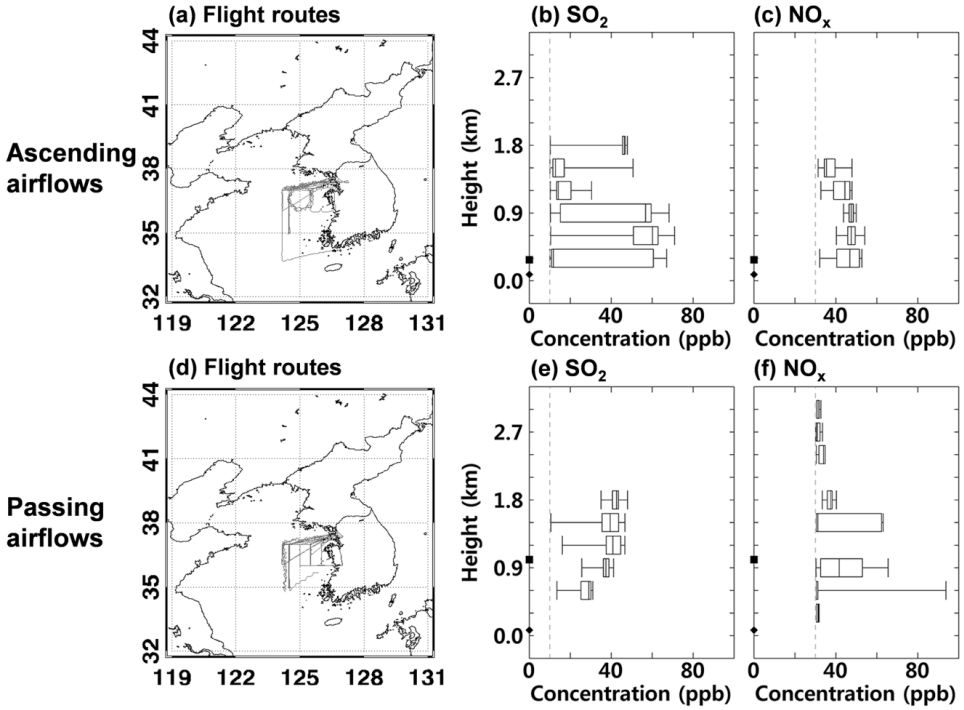

Fig. 3. The flight routes (a, d) and the concentrations of SO_2 (b, e) and NO_x (c, f) which exceed the air quality standards of Seoul in the ascending (9 instances) and passing (12 instances) airflows. The center line of each box plot shows the 50th percentile (median) value and the box encompasses the 25th and 75th percentile of the data. Error bars mark the minimum and maximum values. The gray dashed lines represent the air quality standards of Seoul (SO_2 > 10 ppb, NO_x > 30 ppb). The black squares and diamonds represent the mean PBL height in Osan at 00 UTC and 06 UTC, respectively.

could be diluted by dispersion and/or deposition during the transport. The longer back trajectories in the passing group (i.e., faster wind speed) compared with those in the ascending group (Figs. 2(a) and 2(c)), also support the differences in the concentrations of SO_2 and NO_x.

Meteorological Conditions in the Ascending Group versus the Passing Group

It is well known that the occurrences of the low- and high-pressure systems are closely related with the vertical transport of air pollutants. Therefore, the differences in the pressure patterns between the ascending and passing groups were examined. For the ascending group, considering that the updraft areas of nine airflows differed, weather maps at 12-hour intervals were examined. Fig. 4 displays the synoptic maps on the nine ascending days. In most instances, a surface pressure trough or a low-pressure system was located over eastern China except for a trough in the event shown in Fig. 4(a) where the surface low was located over South Korea. The average of the pressure trough and the low-pressure system is 1017 hPa, approximately 10 hPa below that of the adjacent high-pressure systems. In northeastern China and southwestern Manchuria, where mega metropolises and industrial complexes with large emissions are located, a large quantity of air pollutants could rise up into the FT as the airflows ascend over these regions.

Distributions of atmospheric pressure show three patterns favorable for the ascent of air pollutants: (1) a surface pressure trough, (2) a newly developed low-pressure system, and (3) a migratory low-pressure system over the source regions. First, pressure troughs were located on the updraft areas in four instances (Figs. 4(a), 4(d), 4(h), and 4(i)). These troughs developed into low-pressure systems in 12 to 24 hours over the region or to the east of it (figure not shown), except for the instance in Fig. 4(i) that remained as a trough over the region. Second, newly developed low-pressure systems appear in two instances (Figs. 4(b) and 4(c)) that are wedged between the high-pressure systems. In pressure patterns (1) and (2), the spatial scale of the pressure troughs and the low-pressure systems are relatively small compared with those of the adjacent high-pressure systems. The 700-hPa pressure troughs were located to the west of the surface pressure troughs/low-pressure systems, indicating developing low-pressure systems. Unlike previous studies which suggested that the warm conveyor belt in the mature low-pressure system with fronts may have caused the vertical redistribution of pollutants, these features, shown in five instances (Figs. 4(a), 4(b), 4(c), 4(d), and 4(h)), suggest that the developing low-pressure systems in the early stage without fronts is related to the ascent of air pollutants into the FT. Third, a migratory low-pressure systems passed the region in three instances (Figs. 4(e), 4(f), and 4(g)). In the

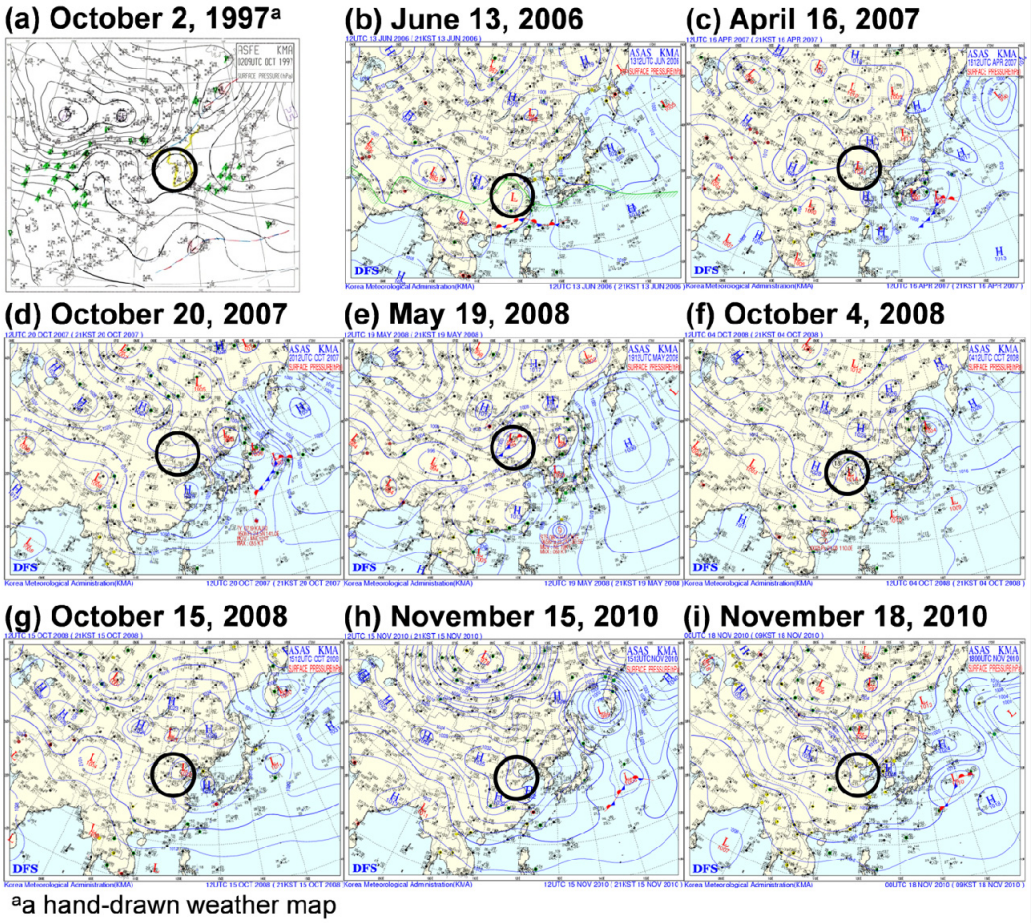

Fig. 4. Synoptic maps on the ascending days of nine instances. The black circles denote the updraft areas of SO_2 and NO_x.

instance of May 19, 2008, the surface low-pressure at the center dropped by 15 hPa in 12 hours. The surface positions of the cold and warm fronts imply that the warm conveyor belt raises the airstream (Bethan *et al.*, 1998), while the mid-latitude cyclone (Fig. 4(e)) is moving eastward. The air pollutants can therefore be uplifted into the FT, concurrent with a rise of the warm conveyor belt from the low level in the bottom left ahead of the warm front. In two instances (Figs. 4(f) and 4(g)), the migratory low-pressure systems were wedged between the high-pressure systems, with a relatively small spatial scale, similar to the features of the developing low-pressure systems. The 700-hPa pressure troughs, located to the west of the surface low-pressure systems, deepened for 24 hours in these three instances. The results show that the mechanisms for transporting air pollutants through the FT and the PBL differ, given that the high-pressure systems are mainly the cause of the accumulation and transport of air pollutants in the PBL (Hatakeyama *et al.*, 2004; Chuang *et al.*, 2008; Wang *et al.*, 2010).

To determine that pollutants at the ground level are lifted into the FT, sea level pressures and weather conditions were examined. We only investigated these for the October 2, 1997 event (Fig. 4(a)), when the airstream rose over South Korea, because the daily emission and concentration data of SO_2 and NO_x, necessary for a detailed analysis, are available only for Seoul. In this instance, the NO_2 concentration (the aircraft did not measure SO_2 on that day), sea level pressure, and the weather conditions observed at stations in Seoul were obtained from the KMA. The NO_2 concentration was 37–43 ppb from September 29 to October 3, above the air quality standards of Seoul. The sea level pressure remained at approximately 1020 hPa and suddenly came down to 1017 hPa on October 3. The one-day gap between the day of the decrease in pressure and the day of ascending in the HYSPLIT model calculations seems to be related with the difference in the data between the station and the reanalysis. Mist and haze were observed throughout the period, implying that the accumulated pollutants were abruptly raised into the FT without dispersion, because of the sudden drop in the atmospheric pressure and the associated low-level updraft. We examined the aerosol optical depth at 550 nm (AOD_{550}) from the TERRA-Moderate Resolution Imaging Spectroradiometer and the air pollution index (API) as an alternative parameter for the remaining eight instances (figure not shown). The concentrations of aerosols were high (i.e., high AOD_{550}) on the ascending areas in eastern China in seven instances, reflecting the emissions from Chinese urban and industrial centers (Song *et al.*, 2008) except in one instance on October 20, 2007. The API at stations near the ascending areas showed that the air was polluted by PM_{10} on the day of ascent, or one day before or after the day of ascent. This result supports the concept that eastern China is the source region of air pollutants in the FT, as measured over the coastal region west of the Seoul metropolitan area.

For the passing group, composites of anomalous geopotential height were examined to identify the pressure patterns conducive to the transport of air pollutants through the FT (Fig. 5). On the –1 day, the pressure systems located in northeastern China showed more pronounced patterns in the upper levels than in those at and near the surface, namely, an upper-level anticyclonic structure. The anomalously high pressure occurred over eastern China and the Yellow Sea at 850 hPa, which is usually just above the PBL, and the anomaly became greater at 700 hPa and 500 hPa. This implies the presence of the ascending motion toward the center of the high-pressure system (Wu *et al.*, 2010), supporting the observed high (> 30 ppb) NO_x concentration at the 3152 m level, shown in Fig. 3(f). On the 0 day, pressure systems at 500, 700, and 850 hPa moved to the east over the Korean peninsula and the 500 hPa geopotential height anomaly at the center was approximately 100 gpm. At 1000 hPa, anomalously low pressure, with a geopotential height anomaly of about –30 gpm at the center, occurred in China, suggesting that the airflow at that level could not descend into the lower altitudes. These features suggest that the airflow in the FT can transport air pollutants over long distances with minimal losses by deposition. Composites of the anomalous vertical velocity (omega) also support these vertical features; the maximum values at 1000 hPa over China and at 500 hPa over Korea are both about –0.08 Pa s^{-1}. Since the number of instances is not sufficient to generalize these mechanisms, further studies are required on the transport patterns of air pollutants observed by aircraft in the FT and on the favorable meteorological conditions.

It seems that air pollutants in the FT often entrain into the PBL to increase the local concentrations. For instance, a high concentration, up to 72 ppb, of NO_x in the FT was measured by the aircraft over the west coastal region of South Korea on October 18, 2007, and the airflow descended on the Seoul metropolitan area after the observation (figure not shown). The mean concentration of NO_2 in Seoul was 43.86 ppb on that day, the highest value in seven days (from –3 day to +3 day). Likewise, the forward trajectories showed the descending patterns toward Korea, Japan, or China for 10 of the 21 instances. This result means that the air quality on the surface is affected by the transboundary pollutants in the FT, as well as those in the PBL and the local emissions. Therefore, continuous monitoring of transported air pollutants in the FT is essential.

SUMMARY

We have analyzed airborne pollutant measurements to examine the high SO_2 and NO_x concentration events in the FT over the coastal region west of the Seoul metropolitan area in South Korea. We selected 21 out of 100 instances, in which the concentrations of SO_2 or NO_x in the FT exceeded the air quality standards of Seoul. These instances were further categorized into an ascending and a passing group over the source regions of the air pollutants, using back trajectory analyses. The meteorological conditions were also examined to find the pressure patterns favorable for the injection of air pollutants into the FT and the subsequent transport of the pollutants, as is schematically depicted in Fig. 6. In five of the nine instances of the ascending group, a low-pressure system in its early stage

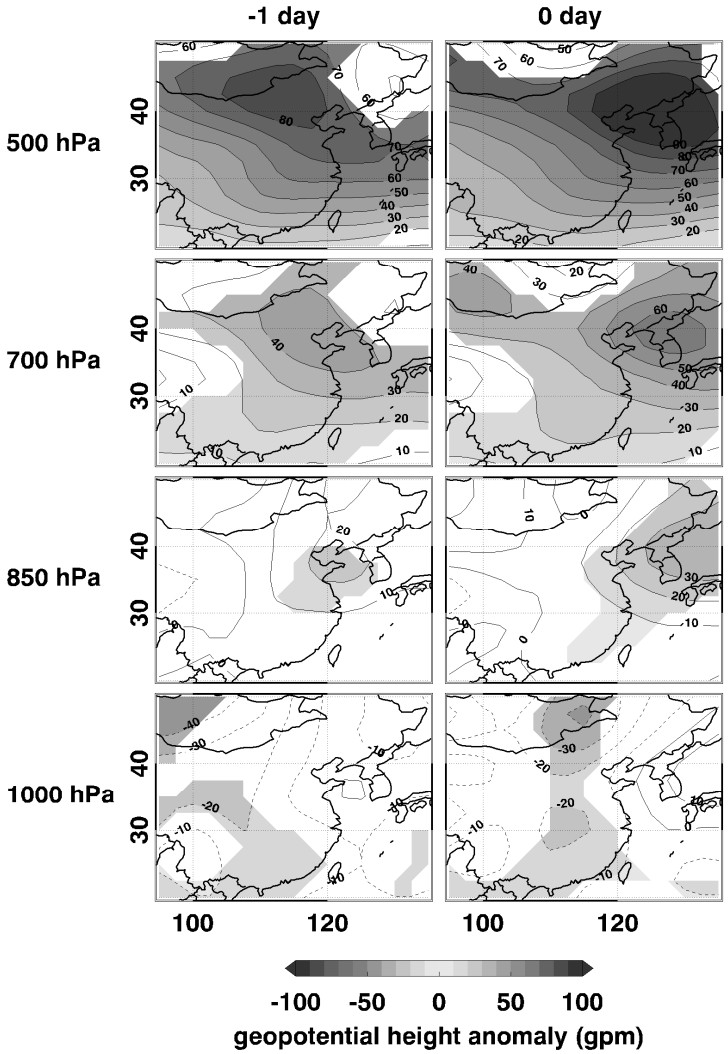

Fig. 5. Composites of anomalous 500, 700, 850, and 1000 hPa geopotential height of 12 passing instances. The left and right panels are composites on the day before and on the day of the flight, respectively. (The shaded area denotes the regions significant at the 90% confidence level.)

was located on the major source regions in eastern China. The smaller spatial scale of the surface low-pressure system compared with the neighboring high-pressure systems and the 700-hPa pressure troughs located to the west of the surface low-pressure system indicated that the low-pressure system was developing. These features suggest that a developing low-pressure system in its early stage, as well as a mature frontal system, creates conditions conducive to the ascent of air pollutants into the FT (Fig. 6(a)). Moreover, this mechanism differs from that in the PBL, that is, the high-pressure system primarily induces the accumulation and transport of air pollutants. The vertical profiles of SO_2 and NO_x for the ascending group indicate that air pollutants could reach a height of approximately 2000 m in only one to three days after upliftment into the FT from the surface. In the 12 instances of the passing group, the upper-level anticyclonic structure helped to uplift the air pollutants within the FT, and an anomalous surface low-pressure system over China prevented the air pollutants from descending into the PBL (Fig. 6(b)). The vertical profiles of SO_2 and NO_x for the passing group imply that these air pollutants could be lifted as high as the 3100 m level. These different features of the two groups suggest that the source regions of transported air pollutants in the FT could vary with atmospheric circulations. Moreover, as the air pollutants in the FT show higher concentrations when transported from the vicinity (e.g., eastern China), it implies that the probability of these pollutants having adverse effects is also higher.

Airborne measurements provide the horizontal and vertical distributions of several chemical components, which are directly and quantitatively observed in the PBL and the FT. Furthermore, using airborne measurements and meteorological data together, we have deduced the basic mechanisms for the injection of air pollutants into the FT and the associated transport of the pollutants. The main uncertainties in this study include; (1) the back trajectories from the HYSPLIT model may not completely correspond with the transport of the air pollutants, (2) the underestimation of PBL height by the bulk Richardson number method, (3) the insufficient number of airborne measurements, and (4)

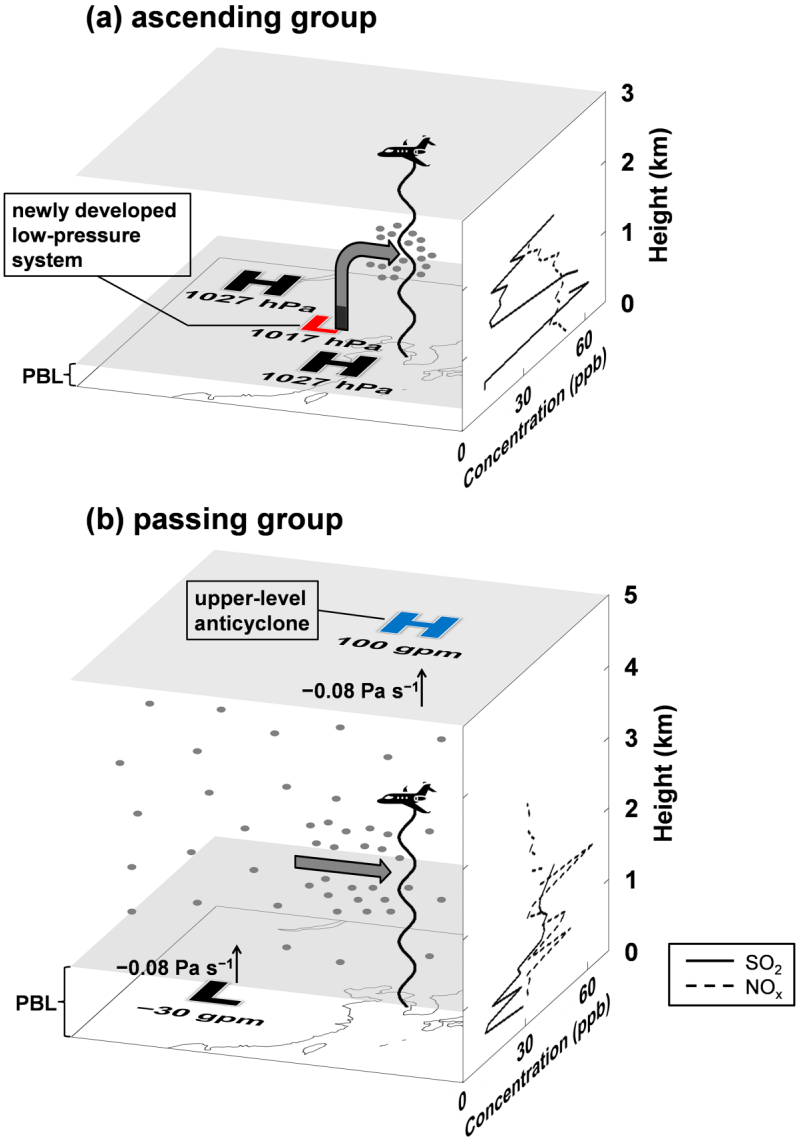

Fig. 6. Schematic diagrams of the pressure patterns in the ascending group (a) and the passing group (b).

the irregular flight plans may also cause uncertainties. Nonetheless, our results from this study emphasize the necessity of monitoring the vertical distribution of air pollutants by using airborne measurements to make provision for the adverse effects of the descending air pollutants from the FT to the surface. The findings in this study will be useful for the prediction of air quality and the forecast of high pollutant concentration events in the future.

ACKNOWLEDGMENTS

This study was funded by the Korea Ministry of Environment (MOE) as "Climate Change Correspondence Program".

SUPPLEMENTARY MATERIALS

Supplementary data associated with this article can be found in the online version at http://www.aaqr.org.

REFERENCES

Bethan, S., Vaughan, G., Gerbig, C., Volz-Thomas, A., Richer, H. and Tiddeman, D.A. (1998). Chemical air mass differences near fronts. *J. Geophys. Res.* 103: 13413–13434.

Chen, P., Quan, J., Zhang, Q., Tie, X., Gao, Y., Li, X. and Huang, M. (2013). Measurements of vertical and horizontal distributions of ozone over Beijing from 2007 to 2010. *Atmos. Environ.* 74: 37–44.

Chin, M., Jacob, D.J., Gardner, G.M., Foreman-Fowler, M.S., Spiro, P.A. and Savoie, D.L. (1996). A global three-dimensional model of tropospheric sulfate. *J. Geophys. Res.* 101: 18667–18690.

China MEP (2012). Ambient Air Quality Standards. GB 3095-2012, China Environmental Science Press, Beijing.

Choi, J.C., Lee, M., Chun, Y., Kim, J. and Oh, S. (2001). Chemical composition and source signature of spring aerosol in Seoul, Korea. *J. Geophys. Res.* 106: 18067–

18074.

Chuang, M.T., Fu, J.S., Jang, C.J., Chan, C.C., Ni, P.C. and Lee, C.T. (2008). Simulation of long-range transport aerosols from the Asian Continent to Taiwan by a southward Asian high-pressure system. *Sci. Total. Environ.* 406: 168–179.

Clerbaux, C., Boynard, A., Clarisse, L., George, M., Hadji-Lazaro, J., Herbin, H., Hurtmans, D., Pommier, M., Razavi, A., Turquety, S., Wespes, C. and Coheur, P.F. (2009). Monitoring of atmospheric composition using the thermal infrared IASI/MetOp sounder. *Atmos. Chem. Phys.* 9: 6041–6054.

Colette, A., Menut, L., Haeffelin, M. and Morille, Y. (2008). Impact of the transport of aerosols from the free troposphere towards the boundary layer on the air quality in the Paris area. *Atmos. Environ.* 42: 390–402.

Cooper, O.R., Parrish, D.D., Stohl, A., Trainer, M., Nedelec, P., Thouret, V., Cammas, J.P., Oltmans, S.J., Johnson, B.J., Tarasick, D., Leblanc, T., McDermid, I.S., Jaffe, D., Gao, R., Stith, J., Ryerson, T., Aikin, K., Campos, T., Weinheimer, A. and Avery, M.A. (2010). Increasing springtime ozone mixing ratios in the free troposphere over western North America. *Nature* 463: 344–348.

Corrigan, C.E., Roberts, G.C., Ramana, M.V., Kim, D. and Ramanathan, V. (2008). Capturing vertical profiles of aerosols and black carbon over the Indian Ocean using autonomous unmanned aerial vehicles. *Atmos. Chem. Phys.* 8: 737–747.

Deeter, M.N., Emmons, L.K., Francis, G.L., Edwards, D.P., Gille, J.C., Warner, J.X., Khattatov, B., Ziskin, D., Lamarque, J.F., Ho, S.P., Yudin, V., Attie, J.L., Packman, D., Chen, J., Mao, D. and Drummond, J.R. (2003). Operational carbon monoxide retrieval algorithm and selected results for the MOPITT instrument. *J. Geophys. Res.* 108: 4399.

Dickerson, R.R., Li, C., Li, Z., Marufu, L.T., Stehr, J.W., McClure, B., Krotkov, N., Chen, H., Wang, P., Xia, X., Ban, X., Gong, F., Yuan, J. and Yang, J. (2007). Aircraft observations of dust and pollutants over northeast China: Insight into the meteorological mechanisms of transport. *J. Geophys. Res.* 112: D24S90.

Ding, A., Wang, T., Xue, L., Gao, J., Stohl, A., Lei, H., Jin, D., Ren, Y., Wang, X., Wei, X., Qi, Y., Liu, J. and Zhang, X. (2009). Transport of north China air pollution by midlatitude cyclones: Case study of aircraft measurements in summer 2007. *J. Geophys. Res.* 114: D08304.

Draxler, R.R. and Rolph, G.D. (2015). HYSPLIT (HYbrid Single-Particle Lagrangian Integrated Trajectory) Model Access via NOAA ARL READY Website (http://ready.arl.noaa.gov/HYSPLIT.php), NOAA Air Resources Laboratory, Silver Spring, MD.

Hatakeyama, S., Takami, A., Sakamaki, F., Mukai, H., Sugimoto, N. and Shimizu, A. (2004). Aerial measurement of air pollutants and aerosols during 20–22 March 2001 over the East China Sea. *J. Geophys. Res.* 109: D13304.

He, H., Li, C., Loughner, C.P., Li, Z., Krotkov, N.A., Yang, K., Wang, L., Zheng, Y., Bao, X., Zhao, G. and Dickerson, R.R. (2012). SO_2 over central China: Measurements, numerical simulations and the tropospheric sulfur budget. *J. Geophys. Res.* 117: D00K37.

Heald, C.L., Jacob, D.J., Park, R.J., Russell, L.M., Huebert, B.J., Seinfeld, J.H., Liao, H. and Weber, R.J. (2005). A large organic aerosol source in the free troposphere missing from current Models. *Geophys. Res. Lett.* 32: L18809.

Heald, C.L., Jacob, D.J., Park, R.J., Alexander, B., Fairlie, T.D., Yantosca, R.M. and Chu, D.A. (2006). Transpacific transport of asian anthropogenic aerosols and its impact on surface air quality in the United States. *J. Geophys. Res.* 111: D14310.

Hess, P.G. and Vukicevic, T. (2003). Intercontinental transport, chemical transformations, and baroclinic systems. *J. Geophys. Res.* 108: 4354.

Holton, J.R. (2004). *An Introduction to Dynamic Meteorology,* Academic press.

Jacob, D.J., Crawford, J.H., Kleb, M.M., Connors, V.S., Bendura, R.J., Raper, J.L., Sachse, G.W., Gille, J.C., Emmons, L. and Heald, C.L. (2003). Transport and Chemical Evolution over the Pacific (TRACE-P) aircraft mission: Design, execution, and first results. *J. Geophys. Res.* 108: 9000, doi: 10.1029/2002JD003276.

Jaffe, D., Anderson, T., Covert, D., Kotchenruther, R., Trost, B., Danielson, J., Simpson, W., Berntsen, T., Karlsdottir, S., Blake, D., Harris, J., Carmichael, G. and Uno, I. (1999). Transport of Asian air pollution to North America. *Geophys. Res. Lett.* 26: 711–714.

Kanamitsu, M., Ebisuzaki, W., Woollen, J., Yang, S.-K., Hnilo, J.J., Fiorino, M. and Potter, G.L. (2002). NCEP–DOE AMIP-II Reanalysis (R-2). *Bull. Am. Meteorol. Soc.* 83: 1631–1643.

Kim, B.G., Han, J.S. and Park, S.U. (2001). Transport of SO_2 and aerosol over the Yellow sea. *Atmos. Environ.* 35: 727–737.

Kim, J. and Mahrt, L. (1992). Simple formulation of turbulent mixing in the stable free atmosphere and nocturnal boundary layer. *Tellus Ser. A* 44: 381–394.

Kim, S.W., Yoon, S.C., Kim, J. and Kim, S.Y. (2007). Seasonal and monthly variations of columnar aerosol optical properties over east Asia determined from multi-year MODIS, LIDAR, and AERONET Sun/sky radiometer measurements. *Atmos. Environ.* 41: 1634–1651.

Koo, Y.S., Kim, S.T., Yun, H.Y., Han, J.S., Lee, J.Y., Kim, K.H. and Jeon, E.C. (2008). The simulation of aerosol transport over East Asia region. *Atmos. Res.* 90: 264–271.

Kotamarthi, V.R. and Carmichael, G.R. (1990). The long range transport of pollutants in the Pacific Rim region. *Atmos. Environ.* 24: 1521–1534.

Kretschmer, R., Gerbig, C., Karstens, U., Biavati, G., Vermeulen, A., Vogel, F., Hammer, S. and Totsche, K.U. (2014). Impact of optimized mixing heights on simulated regional atmospheric transport of CO_2. *Atmos. Chem. Phys.* 14: 7149–7172.

Lee, C., Richter, A., Lee, H., Kim, Y.J., Burrows, J.P., Lee, Y.G. and Choi, B.C. (2008). Impact of transport of sulfur dioxide from the Asian continent on the air quality over Korea during May 2005. *Atmos. Environ.* 42: 1461–1475.

Lee, C., Martin, R.V., van Donkelaar, A., Lee, H.,

Dickerson, R.R., Hains, J.C., Krotkov, N., Richter, A., Vinnikov, K. and Schwab, J.J. (2011). SO_2 emissions and lifetimes: Estimates from inverse modeling using in situ and global, space-based (SCIAMACHY and OMI) observations. *J. Geophys. Res.* 116: D06304.

Lee, H.J., Kim, S.W., Brioude, J., Cooper, O.R., Frost, G.J., Kim, C.H., Park, R.J., Trainer, M. and Woo, J.H. (2014). Transport of NO_x in East Asia identified by satellite and in situ measurements and Lagrangian particle dispersion model simulations. *J. Geophys. Res.* 119: 2574–2596.

Lee, S., Ho, C.H. and Choi, Y.S. (2011). High-PM_{10} concentration episodes in Seoul, Korea: Background sources and related meteorological conditions. *Atmos. Environ.* 45: 7240–7247.

Lee, S., Ho, C.H., Lee, Y.G., Choi, H.J. and Song, C.K. (2013). Influence of transboundary air pollutants from China on the high-PM_{10} episode in Seoul, Korea for the period October 16–20, 2008. *Atmos. Environ.* 77: 430–439.

Lee, S.J., Lee, J., Greybush, S.J., Kang, M. and Kim, J. (2013). Spatial and temporal variation in PBL height over the Korean Peninsula in the KMA operational regional model. *Adv. Meteorol.* 2013: 1–16.

Lee, S.J., Kim, J. and Cho, C.H. (2014). An automated monitoring of atmospheric mixing height from routine radiosonde profiles over South Korea using a web-based data transfer method. *Environ. Monit. Assess.* 186: 3253–3263.

Liu, X., Zhang, Y., Han, W., Tang, A., Shen, J., Cui, Z., Vitousek, P., Erisman, J.W., Goulding, K., Christie, P., Fangmeier, A. and Zhang, F. (2013). Enhanced nitrogen deposition over China. *Nature* 494: 459–462.

Lu, Z., Streets, D.G., Zhang, Q., Wang, S., Carmichael, G.R., Cheng, Y.F., Wei, C., Chin, M., Diehl, T. and Tan, Q. (2010). Sulfur dioxide emissions in China and sulfur trends in East Asia since 2000. *Atmos. Chem. Phys.* 10: 6311–6331.

Mari, C., Evans, M.J., Palmer, P.I., Jacob, D.J. and Sachse, G.W. (2004). Export of Asian pollution during two cold front episodes of the TRACE-P experiment. *J. Geophys. Res.* 109: D15S17.

Miyazaki, Y., Kondo, Y., Koike, M., Fuelberg, H.E., Kiley, C.M., Kita, K., Takegawa, N., Sachse, G.W., Flocke, F., Weinheimer, A.J., Singh, H.B., Eisele, F.L., Zondlo, M., Talbot, R.W., Sandholm, S.T., Avery, M.A. and Blake, D.R. (2003). Synoptic-scale transport of reactive nitrogen over the western Pacific in spring. *J. Geophys. Res.* 108: D208788.

Müller, D., Ansmann, A., Mattis, I., Tesche, M., Wandinger, U., Althausen, D. and Pisani, G. (2007). Aerosol-type-dependent lidar ratios observed with Raman lidar. *J. Geophys. Res.* 112: D16202.

National Institute of Environmental Research (2000–2010). Establishment of Air Pollutants Monitoring System and Cooperating Program for Environmental Conservation in Northeast Asia, National Institute of Environmental Research, http://library.nier.go.kr/search/DetailView.ax?cid=37596.

National Institute of Environmental Research (2011). The Characteristics of Long-Range Transport of Hazardous Air Pollutants (I), National Institute of Environmental Research, http://library.nier.go.kr/search/DetailView.ax?sid=&cid=5511660.

Noh, Y.M., Kim, Y.J., Choi, B.C. and Murayama, T. (2007). Aerosol lidar ratio characteristics measured by a multi-wavelength Raman lidar system at Anmyeon Island, Korea. *Atmos. Res.* 86: 76–87.

Prather, M., Ehhalt, D., Dentener, F., Derwent, R.G., Dlugokencky, E., Holland, E., Isaksen, I.S.A., Katima, J., Kirchhoff, V., Matson, P., Midgley, P.M. and Wang, M. (2001). Atmospheric Chemistry and Greenhouse Gases. In *Climate Change 2001: The Scientific Basis.* Contribution of Working Group I to the Third Assessment Report of the Intergovernmental Panel on Climate Change, Houghton, J.T., Ding, Y., Griggs, D.J., Noguer, N., van der Linden, P.J., Xiaosu, D., Maskell, K. and Johnson, C.A. (Eds.), Cambridge University Press, p. 239–287.

Rolph, G.D. (2015). Real-time Environmental Applications and Display sYstem (READY) website (http://ready.arl.noaa.gov). NOAA Air Resources Laboratory, Silver Spring, MD.

Schmid, B., Flynn, C.J., Newsom, R.K., Turner, D.D., Ferrare, R.A., Clayton, M.F., Andrews, E., Ogren, J.A., Johnson, R.R., Russell, P.B., Gore, W.J. and Dominguez, R. (2009). Validation of aerosol extinction and water vapor profiles from routine Atmospheric Radiation Measurement Program Climate Research Facility measurements. *J. Geophys. Res.* 114: D22207.

Seidel, D.J., Zhang, Y., Beljaars, A., Golaz, J.C., Jacobson, A.R. and Medeiros, B. (2012). Climatology of the planetary boundary layer over the continental United States and Europe. *J. Geophys. Res.* 117: D17106.

Seoul Metropolitan Environment (2014). Evaluation Report of Air Quality in Seoul, Seoul, Korea.

Song, C.H., Park, M.E., Lee, K.H., Ahn, H.J., Lee, Y., Kim, J.Y., Han, K.M., Kim, J., Ghim, Y.S. and Kim, Y.J. (2008). An investigation into seasonal and regional aerosol characteristics in East Asia using model-predicted and remotely-sensed aerosol properties. *Atmos. Chem. Phys.* 8: 6627–6654.

Tsai, F., Chen, G.T.J., Liu, T.H., Lin, W.D. and Tu, J.Y. (2008). Characterizing the transport pathways of Asian dust. *J. Geophys. Res.* 113: D17311.

Tsutsumi, Y., Makino, Y. and Jensen, J.B. (2003). Vertical and latitudinal distributions of tropospheric ozone over the western Pacific: Case studies from the PACE aircraft missions. *J. Geophys. Res.* 108: D84251.

Vardoulakis, S. and Kassomenos, P. (2008). Sources and factors affecting PM_{10} levels in two European cities: Implications for local air quality management. *Atmos. Environ.* 42: 3949–3963.

Vogelezang, D.H.P. and Holtslag, A.A.M. (1996). Evaluation and model impacts of alternative boundary-layer height formulations. *Boundary Layer Meteorol.* 81: 245–269.

Wang, F., Chen, D.S., Cheng, S.Y., Li, J.B., Li, M.J. and Ren, Z.H. (2010). Identification of regional atmospheric

PM_{10} transport pathways using HYSPLIT, MM5-CMAQ and synoptic pressure pattern analysis. *Environ. Modell. Software* 25: 927–934.

Wang, W., Ren, L., Zhang, Y., Chen, J., Liu, H., Bao, L., Fan, S. and Tang, D. (2008). Aircraft measurements of gaseous pollutants and particulate matter over Pearl River Delta in China. *Atmos. Environ.* 42: 6187–6202.

Waters, J.W., Froidevaux, L., Harwood, R.S., Jarnot, R.F., Pickett, H.M., Read, W.G., Siegel, P.H., Cofield, R.E., Filipiak, M.J., Flower, D.A., Holden, J.R., Lau, G.K.K., Livesey, N.J., Manney, G.L., Pumphrey, H.C., Santee, M.L., Wu, D.L., Cuddy, D.T., Lay, R.R., Loo, M.S., Perun, V.S., Schwartz, M.J., Stek, P.C., Thurstans, R.P., Boyles, M.A., Chandra, K.M., Chavez, M.C., Chen, G.S., Chudasama, B.V., Dodge, R., Fuller, R.A., Girard, M.A., Jiang, J.H., Jiang, Y.B., Knosp, B.W., LaBelle, R.C., Lam, J.C., Lee, K.A., Miller, D., Oswald, J.E., Patel, N.C., Pukala, D.M., Quintero, O., Scaff, D.M., Van Snyder, W., Tope, M.C., Wagner, P.A. and Walch, M.J. (2006). The Earth observing system microwave limb sounder (EOS MLS) on the aura Satellite. *IEEE Trans. Geosci. Remote Sens.* 44: 1075–1092.

Welton, E.J., Voss, K.J., Gordon, H.R., Maring, H., Smirnov, A., Holben, B., Schmid, B., Livingston, J.M., Russell, P.B., Durkee, P.A., Formenti, P. and Andreae, M.O. (2000). Ground-based lidar measurements of aerosols during ACE-2: instrument description, results, and comparisons with other ground-based and airborne measurements. *Tellus Ser. B* 52: 636–651.

World Health Organization (2006). WHO Air Quality Guidelines for Particulate Matter, Ozone, Nitrogen Dioxide and Sulfur Dioxide, World Health Organization Regional Office for Europe, Copenhagen.

Wu, R., Wen, Z., Yang, S. and Li, Y. (2010). An interdecadal change in southern China summer rainfall around 1992/93. *J. Clim.* 23: 2389–2403.

Xiao, H., Carmichael, G.R., Durchenwald, J., Thornton, D. and Bandy, A. (1997). Long-range transport of SO_x and dust in East Asia during the PEM B experiment. *J. Geophys. Res.* 102: 28589–28612.

Yu, H., Kaufman, Y.J., Chin, M., Feingold, G., Remer, L.A., Anderson, T.L., Balkanski, Y., Bellouin, N., Boucher, O., Christopher, S., DeCola, P., Kahn, R., Koch, D., Loeb, N., Reddy, M.S., Schulz, M., Takemura, T. and Zhou, M. (2006). A review of measurement-based assessments of the aerosol direct radiative effect and forcing. *Atmos. Chem. Phys.* 6: 613–666.

Zhang, Q., Ma, X., Tie, X., Huang, M. and Zhao, C. (2009). Vertical distributions of aerosols under different weather conditions: Analysis of in-situ aircraft measurements in Beijing, China. *Atmos. Environ.* 43: 5526–5535.

Zhang, W., Zhu, T., Yang, W., Bai, Z., Sun, Y.L., Xu, Y., Yin, B. and Zhao, X. (2014). Airborne measurements of gas and particle pollutants during CAREBeijing-2008. *Atmos. Chem. Phys.* 14: 301–316.

Zhao, B., Wang, S., Dong, X., Wang, J., Duan, L., Fu, X., Hao, J. and Fu, J. (2013). Environmental effects of the recent emission changes in China: Implications for particulate matter pollution and soil acidification. *Environ. Res. Lett.* 8: 024031.

Zhu, A., Ramanathan, V., Li, F. and Kim, D. (2007). Dust plumes over the Pacific, Indian, and Atlantic oceans: Climatology and radiative impact. *J. Geophys. Res.* 112: D1620.

Received for review, June 15, 2015
Revised, September 21, 2015
Accepted, October 14, 2015